Original scientific paper

GENERATION OF SEQUENCES OF STRONG ELECTRIC MONOPULSES IN NITRIDE FILMS

Volodymyr Grimalsky[1], Svetlana Koshevaya[1], Jesus Escobedo-Alatorre[1], Anatoliy Kotsarenko[2]

[1]Center for Investigations on Engineering and Applied Science (CIICAp),
Institute for Investigations on Basic and Applied Science (IICBA),
Autonomous University of State Morelos (UAEM), Cuernavaca, Mor., Mexico.
[2]Faculty of Engineering, Autonomous University of Carmen (UNACAR),
Ciudad Del Carmen, Camp., Mexico

Abstract. *This paper presents theoretical investigation of the excitation of the sequences of strong nonlinear monopulses of space charge waves from input small envelope pulses with microwave carrier frequencies due to the negative differential conductivity in n-GaN and n-InN films. The stable numerical algorithms have been used for nonlinear 3D simulations. The sequences of the monopulses of the strong electric field of 3 – 10 ps durations each can be excited. The bias electric field should be chosen slightly higher than the threshold values for observing the negative differential conductivity. The doping levels should be moderate 10^{16} –10^{17} cm^{-3} in the films of ≤ 2 μm thicknesses. The input microwave carrier frequencies of the exciting pulses of small amplitudes are up to 30 GHz in n-GaN films, whereas in n-InN films they are lower, up to 20 GHz. The sequences of the electric monopulses of high peak values are excited both in the uniform nitride films and in films with non-uniform conductivity. These nonlinear monopulses in the films differ from the domains of strong electric fields in the bulk semiconductors. In the films with non-uniform doping the nonlinear pulses are excited due to the inhomogeneity of the electric field near the input end of the film and the output nonlinear pulses are rather domains.*

Key words: *nitride films, negative differential conductivity, picosecond pulses, nonlinearity*

1. INTRODUCTION

The nitrides GaN, InN are used in the microwave range and the lower part of terahertz (THz) range f = 100 GHz – 1 THz to fabricate powerful active and nonlinear devices like transistors, generation diodes, and integrated power amplifiers [2-12]. Recently it was demonstrated that n-InN possesses the increased values of the negative differential conductivity (NDC), probably the highest ones between the semiconductor materials [13,14]. The space charge waves (SCW) in n-GaN and n-InN films can be amplified due to NDC, when the magnitudes of bias electric fields are higher than the critical, or threshold, ones [15].

The linear amplification of SCW in n-GaN and n-InN films was investigated in the frequency range f < 800 GHz, where the non-local dependence of the electron velocity on the average electron energy was taken into account [15-17]. The typical thicknesses of the films were $2l$ = 0.2 – 1 μm, their lengths were 10 – 50 μm, see Fig. 1. Because the frequency range of amplification of SCW in the nitride films is wide and covers the lower part of THz range, it is of interest to investigate the excitation of strong nonlinear monopulses of picosecond durations without internal carrier frequency [1,18,19]. These monopulses occupy the wide frequency range Δf >100 GHz.

The maximum values of the spatial increments of the linear amplification of SCW in the nitride films achieve at the frequencies f > 50 GHz. Those differ from the bulk crystals where the maximum increments correspond to the zero frequency [20]. Therefore the strong monopulses in semiconductor films with NDC differ from the ordinary domains in the bulk semiconductors [20]. Under the excitation of the domains the electric field out of them is essentially below the threshold value, whereas in the films the electric field out of the monopulses practically does not change and is equal to the bias one [1,18,19]. Moreover, only a single domain can propagate simultaneously within the crystal, and the next domain is excited when the previous one leaves the crystal.

The strong monopulses can be excited when the bias electric field slightly exceeds the critical value of the electric field for NDC and the doping levels are moderate [1,18,19]. Note that the domain regime of operation is not preferable in the bulk Gunn diodes, because of its lower efficiency compared with another regimes, like the limitation of accumulation of space charge one [20].

The most interesting case is the excitation of sequences of strong monopulses from input envelope pulses of small amplitudes with the carrier frequency of the microwave range 10 – 50 GHz. Such an excitation was not considered earlier and is important for the practical needs of the modulation of the optical radiation by SCW in laser devices [21-25]. Under such an excitation the repetition rate of the output monopulses is determined by the input carrier frequency. This paper is devoted to the investigations of the generation of sequences of output strong monopulses under excitation by input microwave pulses of small amplitudes.

In the films the influence of the boundaries on the properties of the films is principal. Namely, at the boundaries the electron mobility can be lower than in the center of the film and, moreover, NDC can be absent at the boundaries due to additional mechanisms of carrier scattering. In the last case the non-uniform doping can be used that is increased in the center of the film x = l and is decreased at the boundaries of the film x = 0, x = $2l$, see Fig. 1. In the present consideration the permittivities below and above the film are ε_l = 4, SiO$_2$, and ε_3 = 1, air.
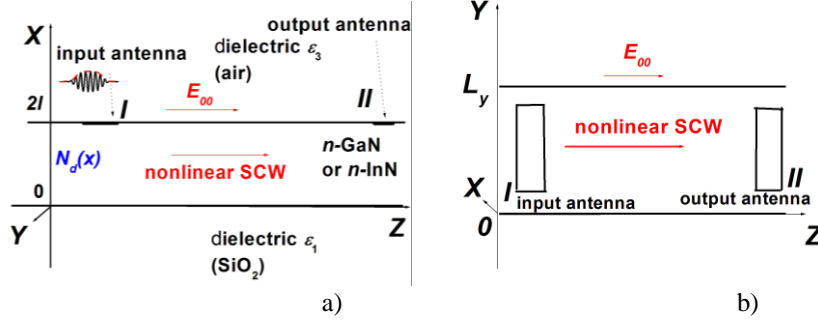
Fig. 1 The geometry of the problem. Parts a), b) are views from different directions. The nitride film occupies the region $0 \leq x \leq 2l,\ 0 \leq y \leq L_y,\ 0 \leq z \leq L_z$. $N_d(x)$ is the non-uniform doping profile. The input antenna is *I*. The nonlinear space charge waves are formed as strong monopulses of picosecond durations at the output antenna *II*. The pulses are generally localized also along *OY* axis.

2. BASIC EQUATIONS

The non-local electron hydrodynamics can be used to investigate nonlinear SCW in the nitride films [1, 15-19, 26, 27]. In this approach the dynamics of the electron gas is described by the full electron concentration *n* in all valleys jointly, the average electron velocity *V*, and by the average electron energy *w*. This model is valid for the nitrides *n*-GaN and *n*-InN and cannot be applied for *n*-GaAs [27], because in the last material the occupation of the different valleys is principally important to calculate the diffusion coefficient. The equations of the balance of the number of electrons, the linear momentum, and of the electron energy are:

$$\frac{\partial n}{\partial t} + div(n\vec{V}) = 0; \quad \frac{d\vec{V}}{dt} \equiv \frac{\partial \vec{V}}{\partial t} + (\vec{V} \cdot \vec{\nabla})\vec{V} = \frac{e\vec{E}}{m^*(w)} -$$

$$\frac{1}{nm^*(w)}\vec{\nabla}(nT) - \vec{V}\nu_p(w); \quad \vec{E} = \vec{E}_0 - \vec{\nabla}\phi;$$

$$\frac{dw}{dt} = e\vec{E} \cdot \vec{V} - \frac{1}{n}\vec{\nabla} \cdot ((n\vec{V} - \kappa\vec{\nabla})T) - (w - w_{00})\nu_w(w);$$

$$where \quad T = \frac{2}{3}(w - \frac{m^*(w)V^2}{2}); \quad \kappa = \frac{5nT}{2m^*\nu_p(w)}.$$

(1)

Here *n* is the total electron concentration, *V* is the average velocity, *w* is the average electron energy; $\nu_p,\ \nu_w$ are the effective relaxation frequencies of the electron momentum and energy, m^* is the effective electron mass, *T* is the electron temperature in energetic units, κ is the electron thermoconductivity coefficient. $w_{00} = 0.039$ eV is the average electron energy at 300 K; $E_{00} \equiv E_{0z}$ is the bias constant electric field. It is assumed that $\nu_p,\ \nu_w,\ m^*$ are the functions of the average electron energy *w*. An influence of the thermoconductivity

on the electron gas dynamics is not essential up to the frequencies $f \leq 2 - 3$ THz [15]. The electron kinetic energy for the investigated processes is one order lower than the average electron energy, so it is $T \approx (2/3)w$.

The utilized dependencies of the drift velocity and the average electron energy on the electric field for the zinc blende n-GaN and for n-InN [28] are presented in Fig. 2. It is assumed that in the non-uniform films NDC at the surfaces is absent, as depicted by the dash curves 1, 2. The results of our investigations are tolerant to changes of the dependencies of the drift velocity at the surfaces of the films.

a)   b)
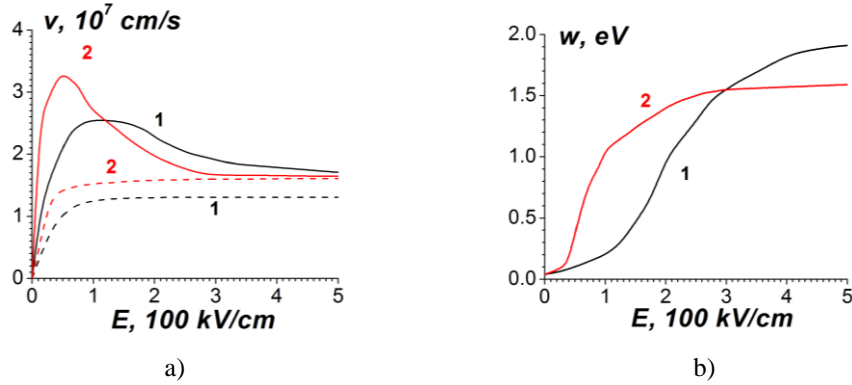
Fig. 2 Parts a), b) are dependencies of the drift velocity v and the average electron energy w on the electric field for the zinc blende n-GaN, solid curve 1, and n-InN, solid curve 2. Dash curves 1 and 2 are the used dependencies $v(E)$ at the boundaries of the n-GaN and n-InN non-uniform films where NDC is absent.

The dependencies of the relaxation frequencies were computed from Eqs. (1) in the stationary case $\partial/\partial t = 0$ [1, 15-19]; the dependencies in Fig. 2, a), b), were used.. Their computed values are $v_p \geq 2 \cdot 10^{13}$ s^{-1} for both nitrides; $v_w \approx 10^{12}$ s^{-1} for InN, $v_w \approx 10^{13}$ s^{-1} for GaN [15]. Thus, it is $v_p >> v_w$. Therefore at the frequencies $f < 1$ THz the inertia of the electron gas can be neglected:

$$\vec{V} \approx \frac{e}{m^* v_p} \vec{E} - \frac{1}{nm^* v_p} \vec{\nabla}(nT) = \mu(w)\vec{E} - \frac{D}{nw} \vec{\nabla}(nw). \tag{2}$$

Here μ, D are the coefficients of the electron mobility and the diffusion:

$$\mu = \frac{e}{m^* v_p}; \quad D = \frac{T}{m^* v_p} \equiv \frac{\mu}{e} T. \tag{3}$$

The relaxation frequency v_w in n-InN is smaller than in n-GaN; this fact limits the frequency range of the amplification of SCW in the n-InN films [15].

Below the processes are considered in the wide frequency range $f \leq 300$ GHz, or with the temporal scales ≥ 3 ps, so the using of Eq. (2) results in the following diffusion-drift equations for the total electron concentration:

$$\frac{\partial n}{\partial t} + \frac{\partial j_x}{\partial x} + \frac{\partial j_y}{\partial y} + \frac{\partial j_z}{\partial z} = 0, \quad j_x = nv_x - D\frac{\partial n}{\partial x};$$

$$j_y = nv_y - D\frac{\partial n}{\partial y}; \quad j_z = nv_z - D\frac{\partial n}{\partial z}; \quad v_x = \mu(E)E_x,$$

$$v_y = \mu(E)E_y, \quad v_z = \mu(E)E_z; \quad \mu(E) \equiv \frac{v}{E}, \tag{4}$$

$$\frac{4}{3v_w(w)}\frac{\partial v}{\partial t} + v = v_d(E), \quad E \equiv (E_z^2 + E_x^2 + E_y^2)^{1/2},$$

$$E_z = E_{00} - \frac{\partial \phi}{\partial z}, \quad E_x = -\frac{\partial \phi}{\partial x}, \quad E_y = -\frac{\partial \phi}{\partial y}.$$

The simplest model of the taking account of the non-local dependence of the drift velocity v is applied here, to estimate the influence of the nonlocality. The characteristic time of nonlocality was calculated in [16,17], it is of about $4/(3 v_w(w))$. In Eqs. (4) $v_d(E)$ is the stationary dependence of the drift velocity on the electric field presented in Fig. 2, a. In the simulations presented below an influence of the nonlocality is not essential, as it has been checked; such an influence results in <1% variations. Thus, the diffusion-drift equation is valid here with the local dependence of the drift velocity v on the electric field E.

The equations for the dynamics of the electron gas should be added by the Poisson equation for the electric field potential. Note that the potential $\phi = \phi_0(x) + \tilde{\phi}(z,x,y,t)$ includes both the stationary part $\varphi_0(x)$ due to the possible non-uniform doping and the variable in time one $\tilde{\phi}$ due to the propagation of SCW:

$$\frac{\partial^2 \phi}{\partial x^2} + \frac{\partial^2 \phi}{\partial y^2} + \frac{\partial^2 \phi}{\partial z^2} = \begin{cases} -\dfrac{e(n - N_d(x))}{\varepsilon_0 \varepsilon_2}, & 0 < x < 2l; \\ 0, & x < 0, \quad x > 2l. \end{cases} \tag{5}$$

The non-uniform doping is considered as:

$$N_d(x) = N_{d0}\exp(-((x-l)/x_d)^2). \tag{6}$$

Here x_d is the scale of the non-uniform doping.

Under the non-uniform doping the stationary concentration $n_0(x)$, the electric potential $\varphi_0(x)$, and the additional electric field $E_0(x)$ have been calculated from the following set of equations:

$$\frac{d^2\phi_0(x)}{dx^2} = -\frac{e}{\varepsilon_0 \varepsilon_2}(n_0(x) - N_d(x)), E_0(x) \equiv -\frac{d\phi_0(x)}{dx};$$

$$n_0(x) = C \cdot \exp(-\frac{e\phi_0(x)}{k_B T_e}), \quad C = \frac{\displaystyle\int_0^{2l} N_d(x)dx}{\displaystyle\int_0^{2l} \exp(-\frac{e\phi_0(x)}{k_B T_e})dx}. \tag{7}$$

Eqs. (7) have been solved by the iterative Newton method, which is analogous to the Gummel one [29]. It yields the rapid convergence; the obtained accuracy is $<10^{-12}$.

The Poisson equation for the variable electric potential of SCW is

$$\frac{\partial^2 \tilde{\phi}}{\partial x^2} + \frac{\partial^2 \tilde{\phi}}{\partial y^2} + \frac{\partial^2 \tilde{\phi}}{\partial z^2} = \begin{cases} -\dfrac{e(n - n_0(x))}{\varepsilon_0 \varepsilon_2}, & 0 < x < 2l; \\ 0, & x < 0, \quad x > 2l. \end{cases} \tag{8}$$

3. LINEAR AMPLIFICATION OF SCW

To investigate the amplification of linear SCW, the solution of linearized Eqs. (4), (8) is searched as the travelling waves:

$$\tilde{n}, \tilde{w}, \tilde{\phi} \sim \exp(i(\omega t - kz)) . \tag{9}$$

The circular frequency $\omega \equiv 2\pi f$ is real here, whereas the longitudinal wave number is complex $k \equiv k' + ik''$. The amplification of SCW occurs when $k'' > 0$.

In the non-uniform films the dependence of the electron mobility on the coordinate x is taken as

$$\mu(x) = \mu_1 - (\mu_1 - \mu_2)\Phi(x),$$
$$\Phi(x) \equiv \exp(-(x/x_0)^2) + \exp(-((2l - x)/x_0)^2). \tag{10}$$

Here μ_1, μ_2 are the mobilities in the center $x = l$ and at the boundaries $x = 0$, $x = 2l$ of the film taken from Fig. 2, a; x_0 is the scale of the non-uniformity of the conductivity. In the center NDC is present whereas at the boundaries it is absent.

In Fig. 3 there are the results of the simulations of the dependencies of the spatial increments of amplification k'' on the frequency f of linear SCW. For all cases the thickness of the films is $2l = 0.5$ μm. This thickness is quite large to provide the using of SCW for the modulation of laser radiation in the waveguides with the nitride films.

The curves 1, 2 correspond to uniform films. The curve 3 is for the film with non-uniform dependence of the electron mobility μ on x, as in Eq. (10), but with the uniform doping. The curves 4, 5 are for both the non-uniform dependence of $\mu(x)$ and the non-uniform doping $N_d(x)$, Eq. (6). Note that the critical field of NDC in n-GaN is $E_c = 1.25 \cdot 10^5$ V/cm, in n-InN it is $E_c = 0.49 \cdot 10^5$ V/cm. In all cases the bias electric field corresponds to relatively small values of NDC, as it is necessary for the excitation of strong electric monopulses in the nonlinear regime [1,18,19]. When the bias field exceeds the value $E_{00} > 1.4 \cdot 10^5$ V/cm in n-GaN and $E_{00} > 0.54 \cdot 10^5$ V/cm in n-InN, the linear increments of amplification increase sharply and under the nonlinear regime the stable monopulses are not excited there [18].

In Fig. 3 the part a) is for n-GaN film. The curve 1 is for the bias electric field $E_{00} = 1.3 \cdot 10^5$ V/cm, the equilibrium electron concentration is $n_0 = N_d = 10^{17}$ cm^{-3}. The curve 2 is for $E_{00} = 1.35 \cdot 10^5$ V/cm, $n_0 = N_d = 5 \cdot 10^{16}$ cm^{-3}. The curve 3 is for the film with non-uniform conductivity with the scale $x_0 = 0.1$ μm (see Eq. 10), $E_{00} = 1.4 \cdot 10^5$ V/cm, $n_0 = N_d = 10^{17}$ cm^{-3}. The curve 4 is for the film with non-uniform conductivity with the scale $x_0 = 0.1$ μm, $E_{00} = 1.3 \cdot 10^5$ V/cm; the scale of the non-uniform doping is $x_d = 0.2$ μm, $N_{d0} = 10^{17}$ cm^{-3}. The curve

5 is for $E_{00} = 1.3 \cdot 10^5$ V/cm, $x_d = 0.2$ μm, $N_{d0} = 1.53 \cdot 10^{17}$ cm^{-3}. The last case corresponds to the value of the electron concentration averaged along OX axis as 10^{17} cm^{-3}.

In the films with the non-uniform conductivity the increments are essentially smaller than in the uniform films. The increments can be increased in the films with the non-uniform doping, i.e. due to the localization of the concentration of the electrons of conductivity in the center of the films near $x = l$.

The analogous results have been obtained for n-InN films, see Fig. 3, b. But the bias electric fields and doping levels are smaller there in comparison with the case of n-GaN films. For all cases the bias electric field is $E_{00} = 0.52 \cdot 10^5$ V/cm. The curve 1 is for the electron concentration $n_0 = N_d = 1.5 \cdot 10^{16}$ cm^{-3}. The curve 2 is for $n_0 = N_d = 2 \cdot 10^{16}$ cm^{-3}. The curve 3 is for the film with the non-uniform conductivity $x_0 = 0.1$ μm, $n_0 = N_d = 2 \cdot 10^{16}$ cm^{-3}. The curve 4 is for the non-uniformly doped films $x_0 = 0.1$ μm, $x_d = 0.2$ μm, $N_{d0} = 2 \cdot 10^{16}$ cm^{-3}. The curve 5 is for $x_0 = 0.1$ μm, $x_d = 0.2$ μm, $N_{d0} = 3.06 \cdot 10^{16}$ cm^{-3} that corresponds to the averaged electron concentration $2 \cdot 10^{16}$ cm^{-3}.

Thus, the typical frequency range of the linear amplification of SCW is of about 100 GHz and more. The maximum values of the increments reach at the frequencies $f = 50 - 150$ GHz in the films with the moderate doping and under the bias fields slightly above the threshold values. At the lengths of the films $L_z \geq 20$ μm it is possible to obtain the amplification of linear SCW $exp(k''L_z) \geq 10$. After the linear amplification stage, SCW are subject to strong nonlinear processes that are investigated below in Section 4.

a)   b)
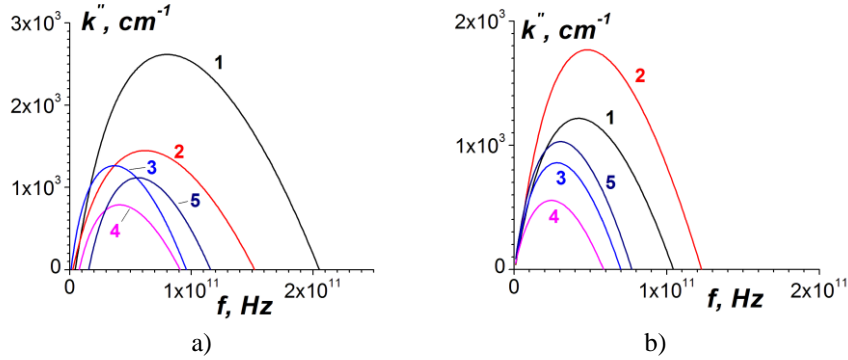
Fig. 3 Spatial increments of amplification of linear SCW. Part a) is for n-GaN fims, b) is for n-InN films. Curves 1, 2 are for uniform films, curve 3 is for non-uniform conductivity but uniform doping; 4, 5 are for non-uniform conductivity and non-uniform doping.

The finite size of SCW along OY axis results in decreasing the increment of amplification [24], i.e. for amplified waves in active media the wave diffraction is equivalent to diffusion.

4. EXCITATION OF SEQUENCES OF NONLINEAR MONOPULSES

The nonlinear dynamics of sequences of SCW nonlinear pulses has been simulated by means of the diffusion-drift equation jointly with the Poisson equation added by boundary conditions Eqs. (4), (8).

The equation for the electron concentration has been solved by the splitting with respect to physical factors [30-32]. The first fractional step is along OX axis, the second one is along OY, the third one is along OZ. The unconditionally stable implicit difference schemes have been used of the second order of approximation. Because the spatial scales along OZ axis and OX, OY ones differ 1 order and more, it is important to preserve the balance of the electric charge at the surfaces, namely to use the integral interpolation method to derive the difference approximations both the volume equations and for the boundary conditions [31].

It is assumed the absence of the surface charge at the boundaries of the film $x = 0$, $x = 2l$. Here the electric boundary conditions are the continuity of the potential and the normal component the electric induction.

At the ends of the film the boundary conditions for the concentration are $n(z=0,x,y)=n_0(x)$ and $\partial n/\partial z(z=L_z) = 0$, the last one corresponds to the Ohmic junctions [20]. The boundary conditions $n(y=0$ or $L_y, z, x) = n_0(x)$ are used at $y = 0$ and $y = L_y$. But in the simulations the film is assumed enough wide, so an influence of the boundary conditions along OY axis is not essential. For the variable electric potential the boundary conditions are $\tilde{\phi} = 0$ at $z = 0$, $z = L_z$.

The Poisson equation for the electric potential $\tilde{\phi}$ has been solved by the fast Fourier transform with respect to z, sine-like, and y, cosine-like ones [30], for real functions. Along OX axis the finite difference method has been used of the second order.

To get a suitable accuracy $\leq 1\%$ the number of the points of the computation grid along OZ axis should be ≥ 512, along OY one it should be ≥ 64, and along OX axis it should be ≥ 50. Because the splitting with respect to physical factors has been applied, i.e. the method of the total approximation, the temporal step has been chosen ≤ 0.1 ps.

The accuracy has been checked by means of 1) checking the approximation of the basic equations at each temporal step; 2) re-simulations with another numbers of the numerical grid points along each axis; 3) using various finite difference approximations, like the central differences and the monotonic schemes; 4) comparison of 3D simulations with 2D ones; 5) comparison of the simulations at the initial linear stage of the dynamics with the analytical results.

The initial pulses of SCW are excited by wide-band planar waveguide; the exciting electric field is at the input antenna:

$$E_z^{exc} = A\exp(-(\frac{t-t_1}{t_0})^2 - (\frac{z-z_1}{z_0})^2 - (\frac{y-L_y/2}{y_0})^2)\cdot\sin(\Omega t). \qquad (11)$$

Here Ω is the carrier circular frequency of the envelope pulse (do not mix with the circular frequency ω from the previous section), z_1, z_0 are the positions of the center of the exciting antenna and its half-width, A is the small input amplitude, $A << E_{00}$. The exciting field is uniform along x, $0 < x < 2l$. For all cases of simulations the thickness of the film is $2l = 0.5$ μm. The similar results have been obtained for the films of the thicknesses $2l \leq 2$ μm. At higher thicknesses the excited pulses are similar to the domains in the bulk Gunn diodes. The lengths of the films are $L_z \geq 30$ μm.

In the case when the bias electric field E_{00} is essentially higher than the critical one and corresponds to the maximum of NDC, the initial strong amplification at the linear stage occurs. But then the amplified pulse deforms at the nonlinear stage of amplification and as a result several powerful oscillations are formed at the output [17]. Therefore, to create stable nonlinear monopulses, the bias electric field should be chosen slightly above the threshold of NDC. Namely in this case the short monopulses are formed at the essentially nonlinear stage

at the output antenna $z = z_2 \le L_z$. Also the moderate doping levels should be applied $n_0 = 3\cdot10^{16} – 10^{17}$ cm^{-3} for n-GaN and $n_0 = 10^{16} – 3\cdot10^{16}$ cm^{-3} for n-InN films.

Below the typical results of numerical simulations are presented. There are dependencies on time t of the variable part of z-component of the electric field of SCW in the center of the output antenna $y = L_y/2$: $\tilde{E}_z(z = z_2, x = 2l, y = L_y/2, t) \equiv E_z - E_{00} - E_0$.

The three cases have been considered. The first one is for the uniform nitride films, the second one is for the films with the non-uniform conductivity, see Eq. (10); the third case is for the films with both the non-uniform conductivity and the non-uniform doping as in Eq. (6). For all the cases the transverse width of the films is $L_y = 100$ μm, the initial transverse width of the input field is $y_0 = 20$ μm.

In Figs. 4-6 there are the results for the uniform films. In all Figs. the left panels are general views, the right ones are the detailed views.

In Fig. 4 the parameters are as follows. There are n-GaN films, the carrier input frequency is $\Omega = 1.5\cdot10^{11}$ s^{-1}. For the parts a), b) the bias electric field is $E_{00} = 1.35\cdot10^5$ V/cm, the constant electron concentration is $n_0 = N_d = 5\cdot10^{16}$ cm^{-3}. The parameters of the input pulse are $A = 3$ kV/cm, $t_1 = 600$ ps, $t_0 = 300$ ps, $z_1 = 10$ μm, $z_0 = 0.5$ μm, see Eq. 11. The length of the film is $L_z = 55$ μm, the output antenna is at $z_2 = 54$ μm. For the parts c), d) they are $E_{00} = 1.3\cdot10^5$ V/cm, $n_0 = N_d = 9\cdot10^{16}$ cm^{-3}; $A = 3$ kV/cm, $t_1 = 600$ ps, $t_0 = 300$ ps, $z_1 = 10$ μm, $z_0 = 0.5$ μm; $L_z = 40$ μm, the output antenna is at $z_2 = 39$ μm. The parts a), c) are general views, b), d) are detailed ones.
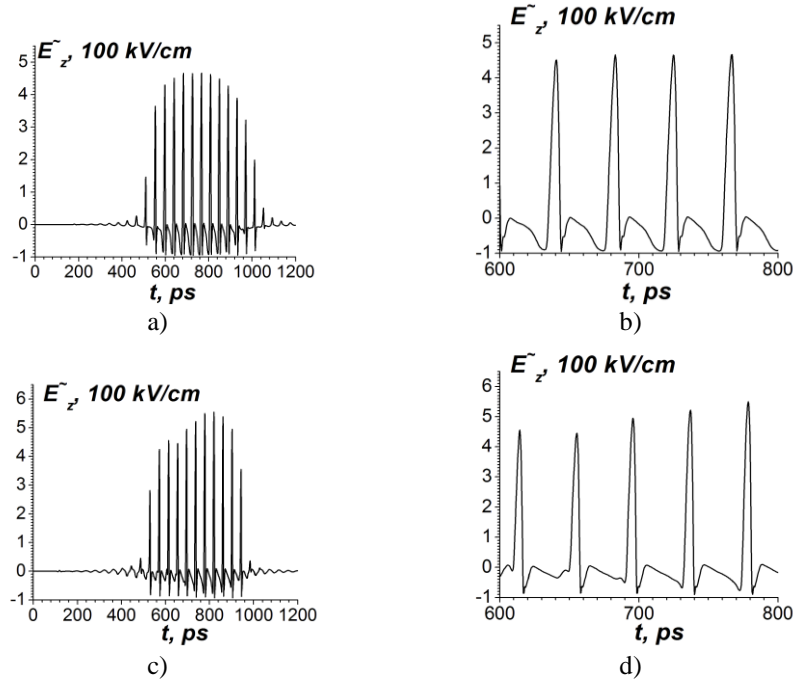
Fig. 4 The shapes of strong electric monopulses at the output antenna in uniform n-GaN film. The input carrier circular frequency is $\Omega = 1.5\cdot10^{11}$ s^{-1}. Parts a), c) are general views, b), d) are detailed ones.

In Fig. 5 there are n-GaN films, the carrier input circular frequency is $\Omega = 2 \cdot 10^{11}$ s^{-1}. The parameters are the same as for Fig. 4, parts a), b).
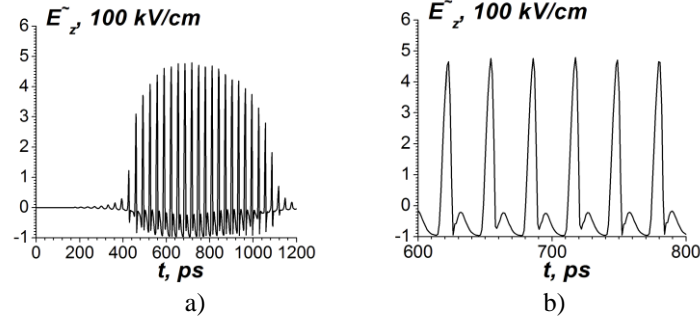
Fig. 5 The shapes of strong electric monopulses at the output antenna in uniform n-GaN film; $\Omega = 2 \cdot 10^{11}$ s^{-1}.

In Fig. 6 there are n-InN films, the carrier input circular frequency is $\Omega = 1.5 \cdot 10^{11}$ s^{-1}. The parameters are $E_{00} = 0.52 \cdot 10^5$ V/cm, $n_0 = N_d = 1.5 \cdot 10^{16}$ cm^{-3}; $A = 3$ kV/cm, $t_1 = 600$ ps, $t_0 = 300$ ps, $z_1 = 10$ μm, $z_0 = 0.5$ μm; $L_z = 60$ μm, the output antenna is at $z_2 = 59$ μm.
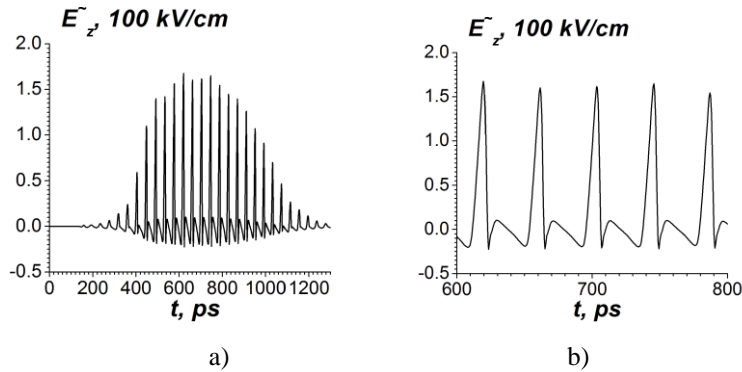
Fig. 6 The shapes of strong electric monopulses at the output antenna in uniform n-InN film; $\Omega = 1.5 \cdot 10^{11}$ s^{-1}.

In Figs. 7, 8 there are the results for the films with the non-uniform conductivity. The scale of the non-uniformity is $x_0 = 0.1$ μm there.

In Fig. 7 there are n-GaN films. The parameters are $E_{00} = 1.4 \cdot 10^5$ V/cm, $n_0 = N_d = 5 \cdot 10^{16}$ cm^{-3}; $A = 2$ kV/cm, $t_1 = 600$ ps, $t_0 = 300$ ps, $z_1 = 10$ μm, $z_0 = 0.5$ μm; $L_z = 50$ μm, the output antenna is at $z_2 = 49$ μm. For the parts a), b) the carrier input circular frequency is $\Omega = 2 \cdot 10^{11}$ s^{-1}; for the parts c), d) it is $\Omega = 1.5 \cdot 10^{11}$ s^{-1}.
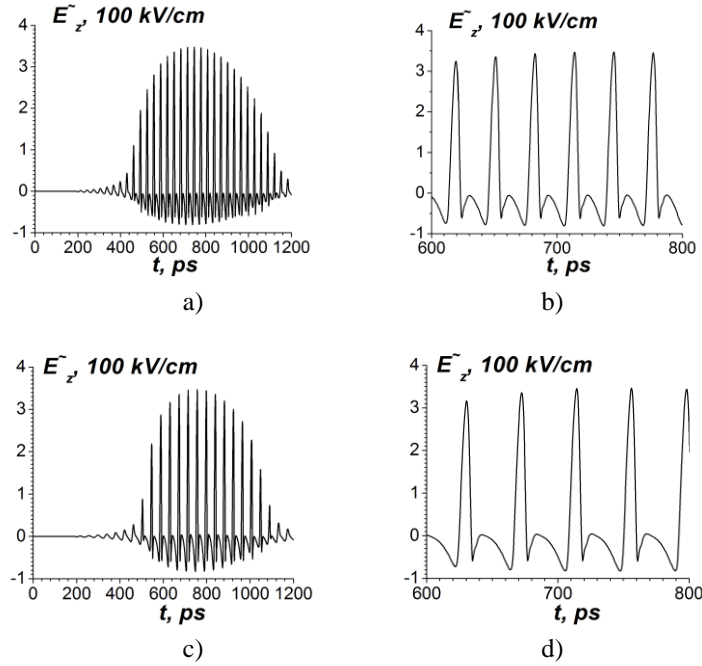
Fig. 7 The shapes of strong electric monopulses at the output antenna in n-GaN film with the non-uniform conductivity.

In Fig. 8 there are n-InN films. The carrier input circular frequency is $\Omega = 1.5\cdot10^{11}$ s^{-1}. The parameters are $E_{00} = 0.53\cdot10^5$ V/cm, $n_0 = N_d = 2\cdot10^{16}$ cm^{-3}; $A = 3$ kV/cm, $t_1 = 600$ ps, $t_0 = 300$ ps, $z_1 = 10$ μm, $z_0 = 0.5$ μm; $L_z = 53$ μm, the output antenna is at $z_2 = 52$ μm.
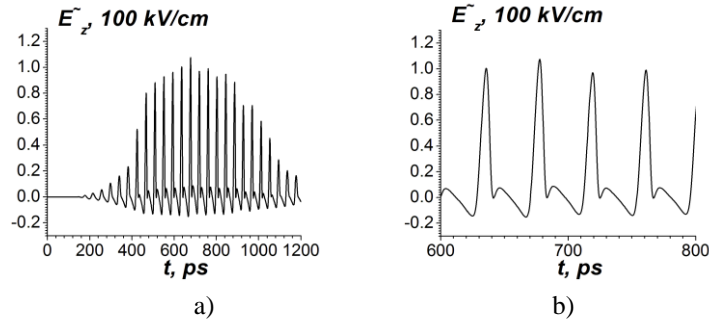
Fig. 8 The shapes of strong electric monopulses at the output antenna in n-InN film with non-uniform conductivity; $\Omega = 1.5\cdot10^{11}$ s^{-1}.

From Figs. 4 – 8 it is seen that the sequences of strong electric monopulses are formed at the output antenna. The maximum values of the output pulses exceed several times the bias electric field E_{00}. The durations of the output monopulses are 3 – 10 ps, so the total frequency range is 100 – 300 GHz. The monopulses are formed practically without any

pedestal and differ from the domains of strong electric field in bulk semiconductors [20]; the domains possess the values of electric fields essentially below the NDC threshold outside of the domain. The repetition rate of the output monopulses is determined by the input carrier circular frequency Ω. Moreover, the peak values of the monopulses repeat the shapes of the envelopes of the input microwave pulses.

In n-GaN films the input carrier circular frequency should be $\Omega \le 2 \cdot 10^{11}$ s^{-1}, in n-InN films it should be $\Omega \le 1.5 \cdot 10^{11}$ s^{-1}. At higher carrier frequencies the behavior of the sequence of output pulses becomes unstable, because there exists the mutual influence of neighboring output monopulses. The peak values of the monopulses are higher in n-GaN films, so namely n-GaN films are preferable for excitations of sequences of strong monopulses, despite the lower values of NDC there. Also the input carrier frequency range is wider in n-GaN films, as mentioned above.

The results of numerical simulations are tolerant to changes of the parameters of input pulses and of the lengths of the films L_z. Under the uniform doping the shapes of the output pulses do not depend on the transverse widths of the input pulse y_0 when $y_0 \ge 20$ μm. At smaller initial widths $y_0 < 20$ μm the maximum values of the electric field of monopulses decrease due to smaller increments of amplification at the linear stage of the SCW dynamics.

In Fig. 9 there are the results for the n-GaN films with both the non-uniform conductivity and the non-uniform doping. The scales of the non-uniform conductivity and the non-uniform doping are $x_0 = 0.1$ μm and $x_d = 0.2$ μm there. The parameters are $E_{00} = 1.3 \cdot 10^5$ V/cm, $n_0 = N_d = 10^{17}$ cm^{-3}; $A = 2$ kV/cm, $t_1 = 600$ ps, $t_0 = 300$ ps, $z_1 = 10$ μm, $z_0 = 0.5$ μm; $L_z = 50$ μm, the output antenna is at $z_2 = 49$ μm.

a)   b)
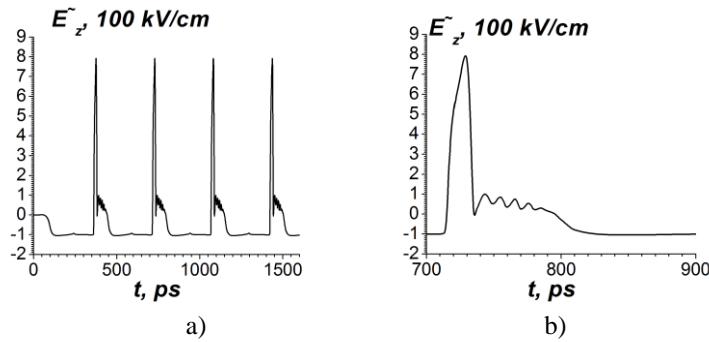
Fig. 9 The shapes of strong electric nonlinear pulses at the output antenna in n-GaN film with both the non-uniform conductivity and with the non-uniform doping; $\Omega = 1.5 \cdot 10^{11}$ s^{-1}.

Under the non-uniform doping the sequences of the monopulses are excited rather due to the non-uniformity of the electric field near the input end of the film $z = 0$ than due to the input field at the exciting antenna. There is a principal difference between the films with the non-uniform doping and with uniform one. In the uniformly doped films the monopulses are not electric domains, whereas under the non-uniform doping the nonlinear pulses possess a similarity to the domains of the strong field in the bulk semiconductors. Namely, the values of the electric field out of the nonlinear pulses are essentially below the threshold ones and the

durations of the nonlinear pulses are essentially longer ≥20 ps. Moreover, in the uniformly doped films the repetition rate of the monopulses at the output antenna is determined by the input carrier circular frequency Ω, whereas under the non-uniform doping the repetition rate is determined by the distance between $z = 0$ and the position of the output antenna $z = z_2$ only.

Note that under the excitation of nonlinear pulses from a single input pulse in the films with non-uniform doping the output pulse can be similar to the strong monopulse like in uniform films [19]. They are shorter and are practically without the pedestal. But in the films with non-uniform doping the sequences of the output pulses are similar to the domains.

The $\tilde{E}_z$ component of the variable electric field is dominating in the nonlinear monopulses. This component is uniform along the thickness of the film i.e. along OX axis.

Because the peak values of the electron concentration are high within the monopulses, the sequences of the strong monopulses can be used for the effective modulation of the electromagnetic radiation of higher part of THz range and of the optical range in the waveguides on the base of the nitride films. In the earlier works such a modulation was considered within the linear regime of amplification of SCW [21-24].

5. CONCLUSIONS

The sequences short strong monopulses of space charge waves of durations $3 - 10$ picoseconds can be excited in the nitride n-GaN и n-InN films of the thicknesses ≤2 μm under the negative differential conductivity when the input signals are the modulated microwave pulses of small amplitudes. The repetition rate of the output monopulses is determined by the carrier frequency of the input microwave pulses. Each monopulse is without the internal carrier frequency and occupies the wide frequency range of about $100 - 300$ GHz. The strong monopulses are formed both in the uniform films and in films with the non-uniform conductivity. These monopulses differ from the domains of the strong electric fields in the bulk semiconductors. The monopulses are realized under the amplification in the essentially nonlinear regime. The bias electric fields should be chosen slightly higher than the thresholds of the negative differential conductivity. The doping levels should be moderate ≤10^{17} cm^{-3}. The typical lengths of the films are $30 - 60$ μm, the widths are ≥ 100 μm.

The n-GaN films are preferable for the excitation of the nonlinear monopulses, because the peak values of the monopulses are higher than ones in n-InN films. Also the carrier microwave circular frequencies at the input can be higher namely in the n-GaN films and are $\Omega \leq 2 \cdot 10^{11}$ s^{-1}, or $f \equiv \Omega/2\pi \leq 30$ GHz. The sequences of strong monopulses can be used for the modulation of the optical radiation in the waveguides on the base of the nitride films.

In the films of the non-uniform doping the sequences of nonlinear pulses are excited due to the electric field inhomogeneity near the input end of the film; the nonlinear pulses are similar to domains of the strong electric field there.

REFERENCES

[1] V. Grimalsky, S. Koshevaya, J. Escobedo-A., and J. Sanchez-S., "Strong electric monopulses in nonuniformly doped nitride films under negative differential conductivity", In Proceedings of the 2019 31st IEEE International Conference on Microelectronics (MIEL), Nis, Serbia, 2019, pp. 83- 86.

[2] Y-S. Lee, *Principles of Terahertz Science and Technology*, Springer, 2009, p. 340.

[3] M. Perenzoni and D. J. Paul, *Physics and Applications of Terahertz Radiation*, Springer, 2014, p. 255.

[4] H.-J. Song, T. Nagatsuma, *Handbook of Terahertz Technologies. Devices and Applications*, Boca Raton, CRC Press, 2015, p. 585.

[5] G. Carpintero, L.E. Garcıa Muñoz, H.L. Hartnagel, S. Preu and A.V. Räisänen, *Semiconductor Terahertz Technology. Devices and Systems at Room Temperature Operation,* John Wiley & Sons, 2015, p. 386.

[6] Y. Nakasha, "Special Section on Terahertz Waves Coming to the Real World" *IEICE Trans. Electron.*, vol. E98.C, no. 12, December 2015.

[7] S. J. Pearton, J. C. Zolper, R. J. Shul and F. Ren, "GaN: processing, defects, and devices", *J. Appl. Phys.*, vol. 86, no 1, pp. 1-79, July 1999.

[8] S. Jain, M. Willander, J. Narayan, and R. Van Overstraeten, "III-nitrides: growth, characterization, and properties", *J. Appl. Phys.*, vol. 87, no. 3, pp. 965-1006, February 2000.

[9] V. Gruzhinskis, P. Shiktorov, E. Starikov, and J. H. Zhao, "Comparative study of 200–300 GHz microwave power generation in GaN TEDs by the Monte Carlo technique", *Semicond. Sci. Technol.*, vol. 16, no 8, pp. 798-805, August 2001.

[10] J. T. Lü and J. C. Cao, "Terahertz generation and chaotic dynamics in GaN NDR diode", *Semicond. Sci. Technol.*, vol. 19, no 4, pp. 451-456, April 2004.

[11] V. I. Timofeyev, E. V. Semenovskaya and O.M. Falieieva, "Electrothermal analysis of GaN power submicron field-effect heterotransistors", *Radioelectron. Commun. Syst.*, vol. 59, no 2, pp. 66–73, February 2016.

[12] A. A. Kokolov and L. I. Babak, "Methodology of built and verification of non-linear EEHEMT model for GaN HEMT transistor", *Radioelectron. Commun. Syst.*, vol. 58, no 10, pp. 435–443, October 2015.

[13] P. Siddiqua, W. A. Hadi, A. K. Salhotra, M. S. Shur and S. K. O'Leary, "Electron transport and electron energy distributions within the wurtzite and zinc-blende phases of indium nitride: Response to the application of a constant and uniform electric field", *J. Appl. Phys.*, vol. 117, no 12, Article ID 125705, June 2015.

[14] W. A. Hadi, P. K. Guram, M. S. Shur and S. K. O'Leary, "Steady-state and transient electron transport within wurtzite and zinc-blende indium nitride", *J. Appl. Phys.*, vol. 113, no 11, Article ID 113709, June 2013.

[15] E. Jatirian Foltides, V. Grimalsky, S. Koshevaya and J. Escobedo-Alatorre, "Amplification of space charge waves in *n*-InN films of THz range", In Proceedings of the IEEE Latin America Microwave Conference LAMC-2016, Puerto Vallarta, Mexico, 2016, pp. 1-3.

[16] V. Grimalsky, S. Koshevaya, M. Tecpoyotl-T. and F. Diaz-A.,"Influence of nonlocality on amplification of space charge waves in n-GaN films", *J. Electromagn. Analysis & Applic. (JEMAA),* vol. 3, no 2, pp. 33-38, February 2011.

[17] V. Grimalsky, S. Koshevaya, I. Moroz, and A. Garcia-B., "Influence of nonlocality on amplification of space charge waves in n-GaN films", In Proceedings of the International Symposium on Physics and Engineering of Microwaves, Millimeter and Submillimeter Waves, Kharkov, Ukraine, 2010, pp. 1-4.

[18] V. Grimalsky, S. Koshevaya, J. Sanchez-S. and Y. Rapoport, "Excitation of short monopulses in nitride films under negative differential conductivity", In Proceedings of the International IEEE Microwaves, Radar, and Remote Sensing Symposium, Kyiv, Ukraine, 2017, pp. 151-154.

[19] S. V. Koshevaya, V. V. Grimalsky, J. Escobedo-Alatorre and M. Tecpoyotl-Torres, "Excitation of short electric monopulse in nitride films with negative differential conductivity", *Radioelectron. Commun. Syst.,* vol. 62, no. 6, pp. 262–270, June 2019.

[20] S. M. Sze and Kwok N. Ng, *Physics of Semiconductor Devices*, Hobokem, Wiley-Interscience, 2007. p. 815

[21] G. E. Chaika, V. N. Malnev and M. I. Panfilov, "Interaction of light with space charge waves", In Proceedings of the SPIE. vol. 2795, 1996, pp. 279-282.

[22] D. G. Sannikov and D. I. Semetsov, "Waveguide interaction of light with amplifying SCW", *Physics of the Solid State (Fizika Tverdogo Tela)*, vol. 49, no. 3, pp. 488-492, March 2007.

[23] S. Yu, Dadoenkova, I. O. Zolotovsky, I. S. Panyaev and D. G. Sannikov, "Modeling the generation of optical modes in a semiconductor waveguide with distributed feedback formed by a space charge wave", *Comput. Opt.,* vol. 44, no 2, pp. 183-188, February 2020.

[24] V. Grimalsky, S. Koshevaya, M. Tecpoyotl-T. and J. Escobedo-A., "Nonlinear interaction of terahertz and optical waves in nitride films", *Terahertz Sci. Technol.,* vol.6, no. 3, pp. 165-176, June 2013.

[25] V. V. Grimalsky, S. V. Koshevaya, Yu. G. Rapoport, "Superheterodyne amplification of electromagnetic waves of optical and terahertz bands in gallium nitride films", *Radioelectron. Commun. Syst.,* vol. 54, no. 8, pp. 401-410, August 2011.

[26] K. Tomizawa, *Numerical Simulation of Submicron Semiconductor Devices*, Boston: Artech House Publ., 1993, p. 356.

[27] A. Garcia-B., V. Grimalsky, E. Gutierrez-D. and S. Koshevaya, "Dispersion relation for two-valley quasi-hydrodynamic models in SCWs propagation in n-GaAs thin films", In Proceedings of the 25th Internatioanl Conference on Microelectronics, Belgrade, Serbia, 2006, pp. 507-510.

[28] M. Levinshtein, S. Rumyantsev and M. Shur, *Properties of Advanced Semiconductor Materials: GaN, AlN, InN*, Wiley, 2001, p. 216

[29] R. Kircher and W. Bergner, *Three-Dimensional Simulation of Semiconductor Devices*, Basel, Birkhauser Verlag, 1991, p. 124.

[30] W. H. Press, S. A. Teukolsky, W. T. Vetterling and B. P. Flannery, *Numerical Recipes in Fortran*, Cambridge, Cambridge Univ. Press, 1997, p. 1486.

[31] A. A. Samarskii, *The Theory of Difference Schemes*, Marcel Dekker Inc., 2001, p. 761.

[32] G. I. Marchuk, *Splitting and Alternating Direction Methods*. In Handbook of Numerical Analysis, Vol. I, Finite Difference Methods, Solution of Equations in R" (Part 1), Amsterdam, Elsevier, 1990, pp. 203-462.